Exploring the effect of Shewanella oneidensis outer membrane redox proteins in the electrochemical response of single blocking impact events

Hassiba Smida, Arthur Langlard, Louis Thomas, Christine Thobie-Gautier, Mohammed Boujtita, Ricardo O Louro, Catarina M Paquete, Estelle Lebègue

Exploring the effect of *Shewanella oneidensis* outer membrane redox proteins in the electrochemical response of single blocking impact events

Hassiba Smida [a], Arthur Langlard [a], Louis Thomas [a], Christine Thobie-Gautier [a], Mohammed Boujtita [a], Ricardo O. Louro [b], Catarina M. Paquete [b], Estelle Lebègue [a,*]

[a] Nantes Université, CNRS, CEISAM, UMR 6230, F-44000 Nantes, France

[b] Instituto de Tecnologia Química e Biológica António Xavier, Universidade Nova de Lisboa, Av. da República, 2780-156 Oeiras, Portugal

[*] Corresponding author: Estelle Lebègue (estelle.lebegue@univ-nantes.fr, Nantes Université, CNRS, CEISAM, UMR 6230, F-44000 Nantes, France)

ABSTRACT

Single blocking impacts electrochemistry was used to explore the redox properties of the outer membrane proteins of the Gram-negative electroactive bacteria *Shewanella oneidensis* on disk-shaped ultramicroelectrodes. We report a comparative study of blocking impact experiments with *E. coli* DH5α and two strains of *S. oneidensis* MR-1 (the wild-type strain SOMR1 and the mutant ΔMtrC ΔOmcA where the MtrC and OmcA outer membrane cytochromes genes were deleted from the genome) based on chronoamperometry measurements recorded in ferrocyanide as a redox probe at +0.8 V vs Ag/AgCl on carbon fiber, Pt and Au ultramicroelectrodes. The data analysis was performed by calculating the change of standard deviation of the background current values measured before and after the first three impact events for each bacterial strain. Compared to others, SOMR1 bacteria increases the magnitude of current fluctuations in the *i–t* curves after the first current step because of the outer membrane redox proteins activity at the polarized ultramicroelectrode

surface. The role of the *S. oneidensis'* outer membrane *c*-type cytochromes redox proteins in the adhesion of electroactive bacteria onto a polarized surface is highlighted by blocking impacts electrochemistry at the single-cell scale for the first time in this work.

Keywords: Shewanella oneidensis, single blocking impact, outer membrane *c*-type cytochromes, background current fluctuations, ultramicroelectrode surface.

1. Introduction

Interest in electroactive bacteria has increased in the last decades, given their promising role in bioelectrochemical systems [1]. In these systems, bacteria interact with electrodes allowing a wide range of applications, including the production of chemicals, biofuels, bioelectricity, and biogas. Electroactive bacteria are living organisms that connect their respiratory metabolism with their extracellular environment by transferring electrons across biological membranes to or from solid materials like metal oxides or electrodes, using periplasmic and membrane proteins [2,3]. This is only possible because of their ability to perform extracellular electron transfer where they can exchange electrons with the electrode directly, or indirectly by using soluble electron shuttles [4–7].

Studies about model electroactive bacteria, including *Shewanella oneidensis* MR-1 (Gram-negative), have demonstrated that extracellular electron transfer pathways consist mainly of periplasmic and membrane-bound multiheme cytochromes, that serve as conduits between intracellular catabolic reactions and extracellular conductive materials, including electrodes [5,8–10]. Several of these proteins, mainly those present at the cell surface, are capable of reducing the soluble electron shuttles used for the indirect electron transfer [7]. The *S. oneidensis'* outer membrane *c*-type cytochromes (Omcs) are not only involved in extracellular electron transfer but are also considered part of the adhesion process of the cells onto electrode surfaces [11–16]. Indeed, the presence of MtrC and OmcA in the outer membrane of *S. oneidensis* is essential for the adhesion and the growth of the cells on a polarized surface, enhancing electron transfer [11,12,14,16]. While MtrC is part of the MtrCAB complex, OmcA is associated with the outer membrane (Fig. 1) intended to move in the outer membrane for the reduction of insoluble compounds [7]. A recent study demonstrated that both MtrC and OmcA have a confined diffusion behavior along the cell's surface, playing an important role in overall electron transport over long distances [17].

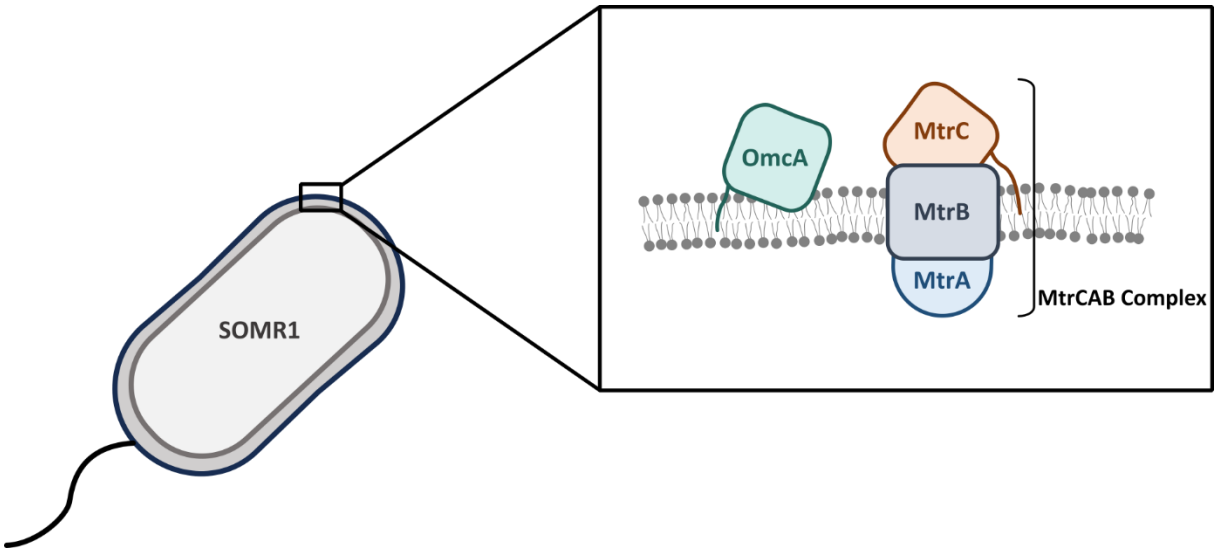

Fig. 1. Localization of the *c*-type cytochromes MtrC and OmcA in the outer membrane of *Shewanella oneidensis* MR-1.

As we previously observed, the adsorption of single *S. oneidensis* MR-1 cells onto the electrode surface strongly depends on the applied potential [18,19]. In our previous study, we reported an electrostatic attraction of the living bacteria toward the ultramicroelectrode (UME) surface polarized at the oxidation potential of the redox probe (potassium ferrocyanide, +0.8 V vs Ag/AgCl) [19]. This behavior is related to the electrostatic interaction between the negatively charged *Shewanella* cells and the positively charged UME surface.

Electrochemical analysis at the single-cell scale has been widely extended to various applications such as biosensing, thanks to the continuous improvement of the instrumentation sensitivity, especially for the electrochemical detection of individual entities [20–22]. In this context, single-entity or nano-impact electrochemistry consists in detecting stochastic impacts of various entities (such as nanoparticles, bacteria or liposomes) in solution onto a polarized UME [20,23–26]. For each collision event, a specific signal is recorded in the chronoamperometry (*i–t*) curve corresponding to an "impact" of a single entity onto the UME surface. The electrochemical nano-impacts method was first reported by Lemay et al. (2004) with the impact of carboxylated latex beads onto Au UME in aqueous solution containing

ferrocene methanol as a redox probe [27]. In this work, single nano-impacts of insulating microspheres cause local decreases of the current at the UME which is polarized at the oxidation potential of the aqueous redox probe. In the recorded chronoamperometry, all of these impacts are noticed as sharp current drops in a staircase fashion, hence the designation "current step". This behavior is called a "blocking impact" and this electrochemical technique represents a promising opportunity for sensing applications and particularly is well adapted to the detection of insulating particles and biotargets such as single bacteria [25,28–31]. Usually, the UME is biased at a potential where the electron transfer reaction is limited by diffusion, in a solution containing the bacterial cells and a redox species. When a bacterium adsorbs onto the UME, it locally stops the diffusive flux of redox species to the electrode, leading to a drop of current (step-shaped transient). Most of the studies dealing with single bacteria blocking collisions were performed with *Escherichia coli* as a model Gram-negative bacterium [29,31–33]. In contrast, our work deals with the single-impact electrochemistry of *S. oneidensis* electroactive bacteria [18,19] and we present herein a comparative study with *E. coli*. For the first time, a significant difference in the background current fluctuations was observed and analyzed in the single blocking impact experiments of these two bacterial strains.

Based on chronoamperograms recorded at the oxidation potential of the ferrocyanide steady-state current (+0.8 V vs Ag/AgCl) at room and cold temperatures, we compared the blocking impact signals of *S. oneidensis* MR-1 (the wild-type strain SOMR1) with its mutant ΔMtrC ΔOmcA (where the MtrC and OmcA outer membrane cytochromes genes are deleted) and *E. coli* DH5α (EC). The analysis of the background current fluctuations before and after a single bacterium collision event (current step signal) on a polarized UME surface (Fig. 2) highlighted the role of the *Shewanella* Omcs redox proteins in the adhesion of the cell.

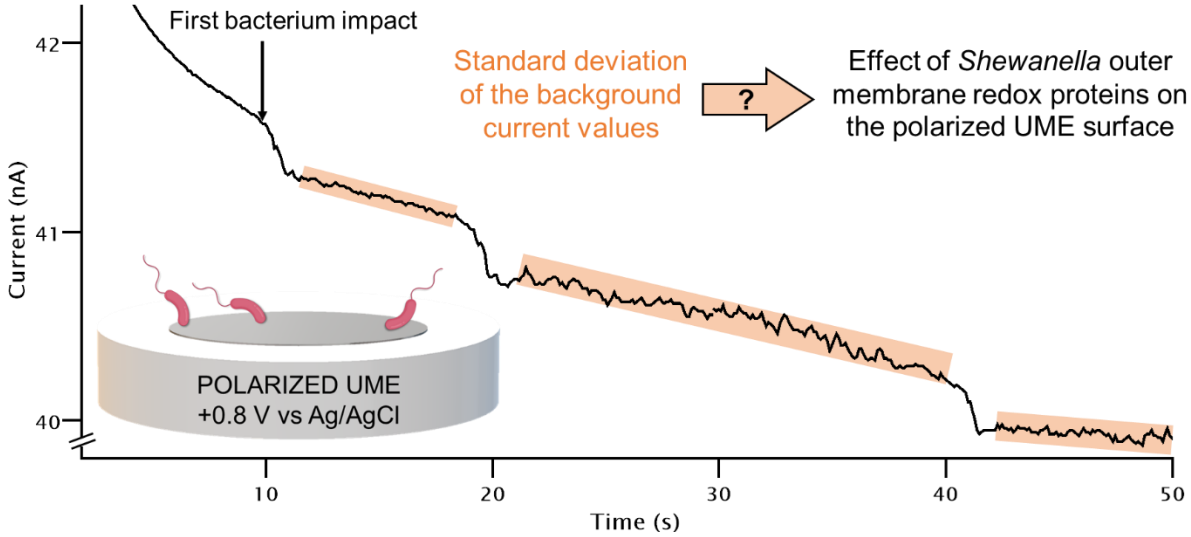

Fig. 2. Analysis of the current fluctuations between single blocking impact events in the *i–t* curve recorded in ferrocyanide aqueous solution and related to the outer membrane redox proteins involved in the bacterial cells' adhesion on the polarized UME surface.

2. Experimental

2.1. Reagents

All chemicals were reagent grade and used as purchased without further purification. Water used in each experiment was deionized water. Potassium ferrocyanide trihydrate (98.5%) was purchased from Acros Organics. Phosphate buffer solution at 1.0 M and pH 7.4 (25 °C) was purchased from Sigma Aldrich and stored at 3 °C. Potassium and sodium chloride were purchased from Sigma Aldrich. Phosphate buffered saline (PBS) used for all experiments was composed of 0.1 M commercial phosphate buffer solution, 50 mM KCl and 50 mM NaCl (pH 7.4 at 25 °C) and was stored at 3 °C. Luria–Bertani (LB) medium, LB agar plates and glycerol were obtained from Sigma Aldrich.

2.2. Bacterial strain and growth conditions

All the manipulations were performed under sterile conditions to avoid contamination with other microorganisms. Pure culture of *Shewanella oneidensis* MR-1 (SOMR1), SOMR1 scarless mutant on both outer-membrane cytochromes genes MtrC and OmcA

(ΔMtrC ΔOmcA) and *Escherichia coli* DH5α (EC) were grown aerobically in LB medium. A single colony collected using a sterile tip from LB agar plates was inoculated into 20 mL of LB liquid medium. The cultures were then allowed to grow overnight on an orbital shaker (STUART, SI600) at 30 °C (for *S. oneidensis*) or 37 °C (for *E. coli*) with a speed of 150 rpm. The growth of the bacterial culture was assessed through the measurement of the optical absorbance at 600 nm using a UV-visible spectrophotometer (Analytikjena SPECORD® 210 PLUS). The optical density at 600 nm (OD600) of the cultures was approximately 4.0, which is consistent with an exponential growth phase [34]. In preparation for the electrochemical impact experiments, the cells underwent an initial washing step with 0.1 M PBS aqueous solution (pH 7.4). Subsequently, they were resuspended in 1 mL of the same buffer and used within a maximum timeframe of 2 hours.

2.3. Electrochemical measurements

Following a procedure similarly reported in our previous work [19], the electrochemical experiments were carried out at room temperature (21 ± 2 °C) and also at cold temperatures (10 ± 3 °C with a bath of cold water) with a three-electrode cell placed in a Faraday cage (BioLogic FC-45) and an SP-300 potentiostat (BioLogic) with an ultra-low current module using the EC-Lab software. For all recorded chronoamperometry *i–t* curves, the sample interval (in sampling time) was 100 ms and the measurement time range was 200 s. For all electrochemical measurements, a Pt wire and an Ag/AgCl (3 M KCl) electrode were respectively used as a counter electrode and a reference electrode. 10 µm-diameter Pt and 12.5 µm-diameter Au disk UMEs from CH Instruments, and a 7 µm-diameter carbon fiber (CF) disk UME from BASi were used as working electrodes. Before each electrochemical experiment, the Pt, Au and CF UMEs were mechanically polished using wetted fine grit silicon carbide paper from Struers (4000-grit SiC) and washed in water. The solution of 50 mM $K_4Fe(CN)_6$ and 0.1 M PBS at pH = 7.4 in the electrochemical cell was

degassed by bubbling N_2 for 5 min before each measurement. The UME was then immersed in the solution of the electrochemical cell, connected as a working electrode and the electrochemical measurement was launched straight away in a matter of a few seconds (max. 5 s of elapsed time). The concentration of washed bacteria in the electrochemical cell was estimated at approximately 10^9 cells mL^{-1} (~2 pM) after dilution of the stock solution with OD600 = 4.0 [35].

2.4. Electrochemical data analysis

For the three first current step signals corresponding to the bacterium blocking impacts recorded in the *i–t* curve, the analysis of the current fluctuations before and after each impact event was performed. This was performed by computing the standard deviation of the current values in the *i–t* curve over 5 s before and after the current step signal for the three first impact events (Fig. 3). Additionally, a subtraction of the baseline was performed to straighten up the values so that only high-frequency fluctuations were measured by the standard deviation, while slow trends were ignored (Fig. S1). All data collected and calculations performed were reported in a spreadsheet file provided in Supplementary Materials (Appendix: Background current SD analysis).

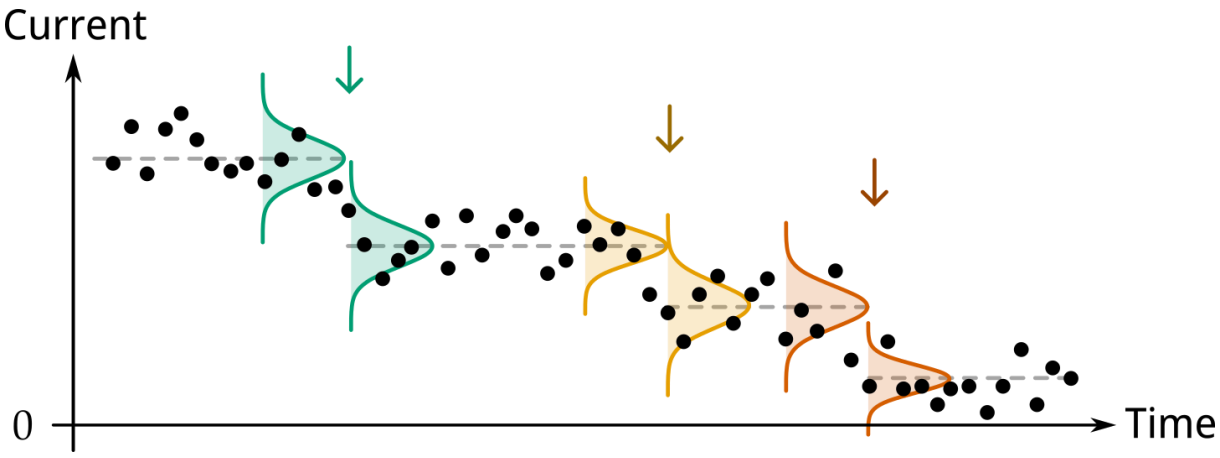

Fig. 3. Diagram representing the data treatment of the current fluctuations for the three first current step signals (indicated by arrows) in the chronoamperometry measurement. The

standard deviation of each plateau (before and after each bacterium impact event) is illustrated by shaded Gaussian curves.

3. Results and discussion

All blocking impact experiments presented in this study were performed by recording a chronoamperometry measurement at the steady-state current oxidation potential of ferrocyanide (+0.8 V vs Ag/AgCl) in an aqueous solution composed of 50 mM $K_4Fe(CN)_6$ and 0.1 M PBS at pH 7.4. As previously reported, before the blocking impact measurements, cyclic voltammetry and *i–t* curves were recorded in a bacteria-free solution in order to check the steady-state current of the working UME according to its size and the concentration of the redox probe [18,19]. Once these control experiments were performed, successive additions of the bacterial cells sample (between 20 and 80 µL) in the electrochemical cell containing 2 mL of the aqueous redox solution were carried out to reach an optimal impact frequency. Indeed, since the analysis of data required the spacing of bacterium impact events in the first three collision signals to be more than 5 seconds, a high collision frequency, related to a concentrated bacterial presence, was not appropriate.

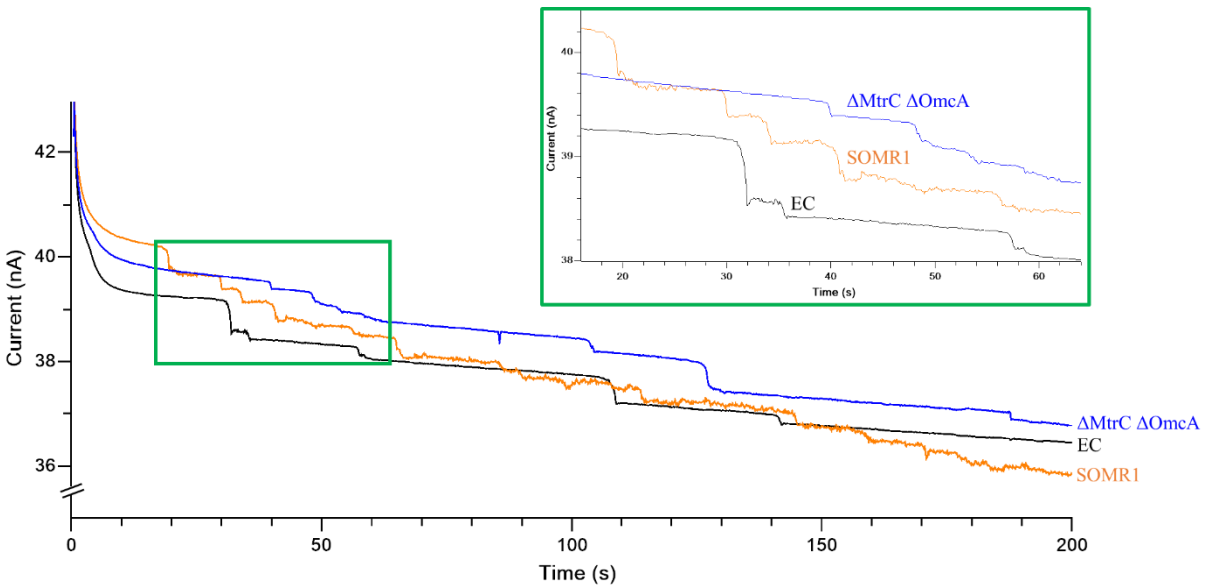

Fig. 4. *i–t* curves recorded on a 7 µm-diameter CF UME at +0.8 V vs Ag/AgCl in 2 mL of 50 mM $K_4Fe(CN)_6$ 0.1 M PBS at pH 7.4 under an inert atmosphere at room temperature, in the presence of ~10^9 cells of EC (black), SOMR1 (orange) and ΔMtr*C* ΔOmcA (blue).

Typical *i–t* curves recorded on 7 µm-diameter CF UME in the presence of about 10^9 cells of EC (black), SOMR1 (orange) and ΔMtrC ΔOmcA (blue) are shown in Fig. 4. As expected in these electrochemical blocking impact experiments, several current step signals were observed, corresponding to single bacterium impact events onto the UME surface [18,19,29,31–33]. The same behavior was observed in the *i–t* curves recorded on 10 µm-diameter Pt and 12.5 µm-diameter Au UMEs as working electrodes (Fig. S2). The difference in the collision frequency (higher for SOMR1) is probably due to a difference in the bacteria concentration in the electrochemical cell rather than a difference in the bacterium surface potential, which is quite close for the negatively-charged EC and SOMR1 cells at pH 7 [36–38]. By focusing on the impact event signals, the current step magnitude values (Δi_{ss}) were similar for the three strains and averaged around 250 pA for EC, SOMR1 and ΔMtrC ΔOmcA bacteria in the *i–t* curves recorded on CF UME (200 pA and 120 pA on Pt and Au UMEs, respectively). Note that, in the present study, only current steps with a current drop at least three times higher than the noisy current fluctuations were considered as collision events. The current step magnitude in electrochemical blocking impact experiments depends on several parameters such as the entity position on the UME surface (edge effect) and the sizes of both the disk UME and the adsorbed entities [28,39,40]. Current steps caused by *E. coli* and *S. oneidensis* had similar magnitudes, as expected from their close shapes and morphologies (rod-shaped bacillus bacteria). Furthermore, the duration of a single cell impact event was virtually always less than 1 s, which is also in agreement with our previous work [19]. The UME surface materials are not critical parameters in single bacteria impacts, as suggested by a similar behavior observed in the different *i–t* curves (Fig. 4 and Fig. S2) and by our previous results [19].

The most significant difference in the *i–t* curves presented in Fig. 4 was the stronger fluctuations of the background current for the SOMR1 strain (orange *i–t* curve) after the first impact events (in the first minute). Indeed, the background current wanes evenly between steps over the duration of the measurement (Fig. 4) for EC (black curve) and ΔMtrC ΔOmcA (blue curve), while with SOMR1 (orange curve) intense fluctuations appear as the number of impacts increases. This qualitative observation can be explained by the different behavior of the adsorbed SOMR1 bacterial cells on the polarized UME because of their Omcs redox proteins. To study this further, this phenomenon was quantitatively investigated by analyzing the standard deviation of the background current values before and after the first three impact events in the *i–t* curves of the three strains. First, a selection of suitable *i–t* curves recorded on CF, Pt and Au UMEs in the presence of EC, SOMR1 and ΔMtrC ΔOmcA bacteria was carried out in order to be able to analyze the current fluctuations between the first three current step signals (Fig. S3). The standard deviation values of the background current values before the first and after the third bacterium impact events of the *i–t* curves recorded on CF, Pt and Au UMEs in the presence of EC, SOMR1 and ΔMtrC ΔOmcA bacteria are summarized in Table 1. Given that the SD values strongly depend on the wear of the UME surface after repeated polishing, only its order of magnitude and the variation between the first and the third bacterium impact events were compared (Table 1). Indeed, the SD value of the background current was usually about 5 ± 3 pA in our experimental conditions, hence we considered that an increase of the SD values superior to three times this initial value (~15 pA) was significant and related to the single bacteria collisions. Moreover, the very discrete nature of charge carriers causes unavoidable fluctuations of current described by the SD $\sigma_i = \sqrt{i\, q_e\, f_{bw}}$. (shot noise) [41]. Considering a current i of 40 nA, this value reaches $\sigma_i = \pm 0.25$ pA for our bandwidth of $f_{bw} = 10$ Hz. As expected, SD values of measured currents are higher because of the additional instrumental noise.

Table 1

Standard Deviation (SD) values of the background current values determined before the first and after the third bacterium impact events of the *i–t* curves recorded on 7 µm-diameter CF, 10 µm-diameter Pt and 12.5 µm-diameter Au UMEs at +0.8 V vs Ag/AgCl in 2 mL of 50 mM $K_4Fe(CN)_6$ 0.1 M PBS at pH 7.4 under an inert atmosphere at room temperature, in the presence of ~10^9 cells of EC, SOMR1 and ΔMtrC ΔOmcA (Fig. S3).

UME	SD (pA)	EC	SOMR1	ΔMtrC ΔOmcA
CF	Before step 1	6	7	1
	After step 3	7	15	4
Pt	Before step 1	3	4	2
	After step 3	2	46	15
Au	Before step 1	4	3	3
	After step 3	5	28	8

For EC bacteria on all three (CF, Pt and Au) UMEs, no significant change was observed for the current fluctuations (SD changes ranged between -1 and +1 pA) before the first and after the third current steps in the *i–t* curves recorded. This suggested that EC cells did not move on the polarized UME surface after the adsorption following the single impact. In contrast, a significant difference between SD values before the first impact (between 3 and 7 pA) and after the third impact (between 15 and 46 pA) was observed for SOMR1 cells. This result could be explained by a different adhesion behavior of the adsorbed SOMR1 electroactive bacteria at the polarized UME. To evaluate if this effect was due to the presence of the Omcs redox proteins at the cell surface, the ΔMtrC ΔOmcA strain was also studied. The increase of SD values before the first (between 1 and 3 pA) and after the third (between 4 and 15 pA) current steps observed for this strain was significantly lower than that observed for native SOMR1. This indicates that the adhesion behavior of adsorbed SOMR1 bacteria on the polarized UME surface is related to the Omcs redox proteins that probably move in the outer membrane of the cells under the polarization effect. The increase of the current

fluctuations for SOMR1 collisions could be also related to a current flow at the cell surface due to the presence of redox proteins, even if our experimental conditions (under aerobic conditions and without the presence of a carbon source) hinder the cells from growing and producing electrons that can be transferred to the electrodes.

In order to investigate if the increase of the current fluctuations in the *i–t* curves recorded in the presence of SOMR1 was due to the cells' mobility on the polarized UME surface, electrochemical blocking impact experiments were performed at cold temperatures (10 ± 3 °C). In these experimental conditions, the current fluctuations related to the mobility of SOMR1 bacteria or Omcs redox proteins onto the polarized UME surface should be much lower than at room temperature (21 ± 2 °C) due to the cells' reduced activity.

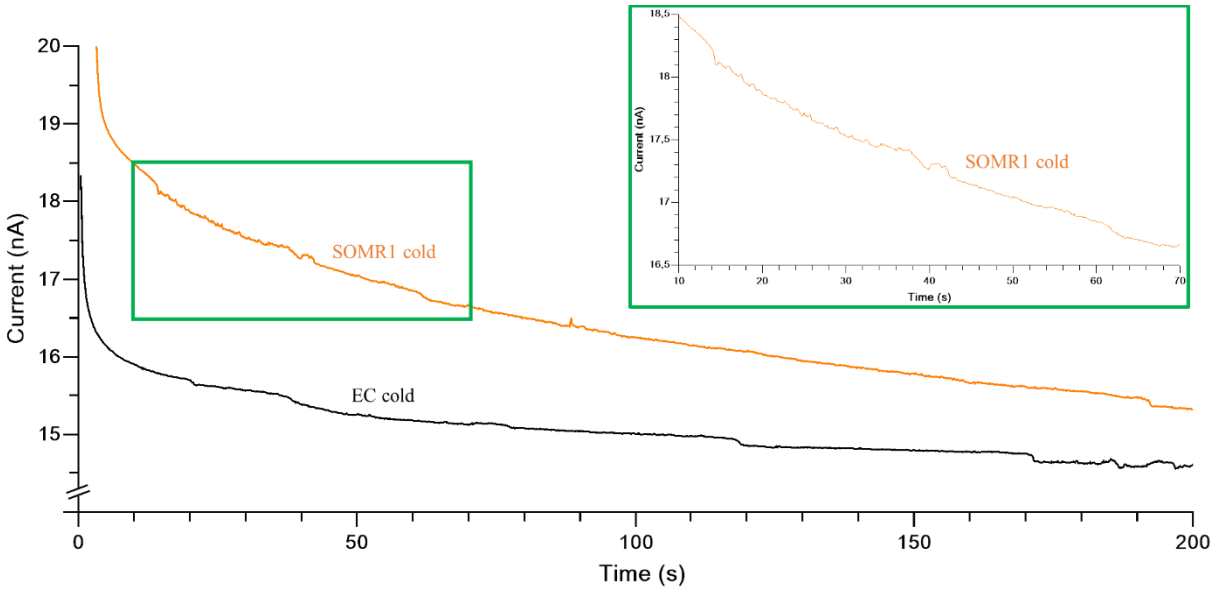

Fig. 5. *i–t* curves recorded on a 7 µm-diameter CF UME at +0.8 V vs Ag/AgCl in 2 mL of 50 mM $K_4Fe(CN)_6$ 0.1 M PBS at pH 7.4 under an inert atmosphere at cold temperatures, in the presence of ~10^9 cells of EC (black) and SOMR1(orange).

Table 2

Standard Deviation (SD) values of the background current values determined before the first and after the third bacterium impact events of the *i–t* curves recorded on 7 µm-diameter CF, 10 µm-diameter Pt and 12.5 µm-diameter Au UMEs at +0.8 V vs Ag/AgCl in 2 mL of 50 mM $K_4Fe(CN)_6$ 0.1 M PBS at pH 7.4 under an inert atmosphere at cold temperatures, in the presence of ~10^9 cells of EC and SOMR1 (Fig. S4).

UME	SD (pA)	EC cold	SOMR1 cold
CF	Before step 1	3	4
	After step 3	7	3
Pt	Before step 1	2	6
	After step 3	4	7
Au	Before step 1	3	9
	After step 3	5	6

In Fig. 5, the *i–t* curves recorded on 7 µm-diameter CF UME in the presence of ~10^9 cells of EC (black curve) and SOMR1 (orange curve) are presented. The SD values of the background current values determined from the corresponding measurements (Fig. 5 for CF UME and Fig. S4 for Pt and Au UMEs) are reported in Table 2. At cold temperatures, the overall current was lower in the *i–t* curves (because current decreases with the temperature), thus the current step magnitude of impact events (between 70 and 90 pA for the three UMEs) was also lower for the three strains. While the SD values (Table 2) determined from *i–t* curves recorded in the presence of EC bacteria were in the same order of magnitude (between 2 and 7 pA) as those at room temperature, the values observed for SOMR1 were different (Fig. S5). For SOMR1 bacteria no significant change of the background current SD (between 3 and 9 pA) before the first and after the third current steps in the *i–t* curves recorded on CF, Pt and Au UMEs was observed at cold temperatures. This result demonstrates that the increase of the current fluctuations observed in the *i–t* curves after the first impact events of single SOMR1 cells at room temperature is indeed related to the adhesion behavior of adsorbed bacteria and the mobility due to the Omcs redox proteins onto the polarized UME surface. It is the first time that the role of *Shewanella*'s Omcs proteins in the bacteria adhesion onto a polarized surface is demonstrated by blocking impacts electrochemistry at the single-cell scale. This study highlights the difference in the electrochemical response of single blocking impact experiments between *E. coli* and *S. oneidensis*, attributed to variations in the redox properties at the cell surface of *Shewanella*.

4. Conclusions

In this work, a comparative study of two Gram-negative bacteria (*E. coli* and *S. oneidensis*) by single blocking impacts electrochemistry was conducted. Chronoamperometry measurements (*i–t* curves) were recorded at +0.8 V vs Ag/AgCl on 7 μm-diameter carbon, 10 μm-diameter Pt and 12.5 μm-diameter Au UMEs in an aqueous solution of 50 mM $K_4Fe(CN)_6$ 0.1 M PBS at pH 7.4 in the presence of three bacteria strains. The data collected for EC and two strains of *S. oneidensis* (the wild-type strain SOMR1 and the mutant ΔMtrC ΔOmcA with the MtrC and OmcA outer membrane cytochromes genes deleted) showed similarities in terms of current step signal magnitude related to the similar shape and size of *E. coli* and *S. oneidensis* bacterial cells. The most significant result of this study was the difference in the current fluctuations obtained with the different strains. Our analysis of the standard deviation of the background current values before and after the three first impact events revealed a different trend for SOMR1 bacteria. Contrary to EC and the mutant ΔMtrC ΔOmcA, which presented stable background currents during the 200 s *i–t* measurement, intensification of the current fluctuations could be observed for SOMR1. Based on supplemental single blocking impact experiments performed at cold temperatures, the increase of the current fluctuations after the first impacts of SOMR1 bacteria at room temperature was assigned to the different adhesion behavior of the adsorbed cells at the polarized electrode surface. This behavior is absent for the *Shewanella* mutant lacking MtrC and OmcA, demonstrating that these Omcs, usually involved in the adhesion properties of this electroactive bacterium, are responsible for the increase of the current fluctuations in the *i–t* curves recorded at room temperature. We suggest that single blocking impacts electrochemistry may be an original and useful tool for investigating *Shewanella* redox proteins in regard to the cell's mobility and adhesion onto a polarized surface. This is important to understand the significance of these proteins not only for electron transfer but

also for the adhesion process to electrodes. This study should be extended to other types of electroactive bacteria.

CRediT authorship contribution statement

Hassiba Smida: Data curation, Formal analysis, Investigation, Methodology, Visualization, Writing – review & editing. Arthur Langlard: Formal analysis, Investigation, Methodology, Visualization, Writing – review & editing. Louis Thomas: Data curation, Formal analysis, Investigation. Christine Thobie-Gautier: Investigation, Writing – review & editing. Mohammed Boujtita: Investigation, Writing – review & editing. Ricardo O. Louro: Investigation, Methodology, Writing – review & editing. Catarina M. Paquete: Conceptualization, Funding acquisition, Methodology, Writing – original draft, Writing – review & editing. Estelle Lebègue: Conceptualization, Funding acquisition, Methodology, Supervision, Writing – original draft, Writing – review & editing.

Declaration of Competing Interest

The authors declare that they have no known competing financial interests or personal relationships that could have appeared to influence the work reported in this paper.

Data availability

Data will be made available on request.

Acknowledgements

The authors thank Prof. Johannes Gescher for providing the ΔMtrC ΔOmcA *Shewanella* strain. This work was supported by the Pays de la Loire Regional Council (Rising stars program, *e-NANOBIO*) and the French National Research Agency (ANR-21-CE42-0007-01, *ELIPOX*). The authors acknowledge the PHC PESSOA program (project number: 47857YM), funded by the French Ministry for Europe and Foreign Affairs, the French Ministry for Higher Education and Research and the Portuguese Foundation for Science and Technology. Financial support was provided by the Portuguese foundation for science and technology to MOSTMICRO-ITQB base funding with references UIDB/04612/2020 and UIDP/04612/2020, and LS4FUTURE Associated Laboratory (LA/P/0087/2020).

Supplementary materials

Supplementary material associated with this article can be found, in the online version.

References

[1] D. Pant, A. Singh, G.V. Bogaert, S.I. Olsen, P.S. Nigam, L. Diels, K. Vanbroekhoven, Bioelectrochemical systems (BES) for sustainable energy production and product recovery from organic wastes and industrial wastewaters, RSC Adv. 2 (2012) 1248–1263. https://doi.org/10.1039/C1RA00839K.

[2] B.E. Logan, K. Rabaey, Conversion of Wastes into Bioelectricity and Chemicals by Using Microbial Electrochemical Technologies, Science 337 (2012) 686–690. https://doi.org/10.1126/science.1217412.

[3] A. Sydow, T. Krieg, F. Mayer, J. Schrader, D. Holtmann, Electroactive bacteria—molecular mechanisms and genetic tools, Appl. Microbiol. Biotechnol. 98 (2014) 8481–8495. https://doi.org/10.1007/s00253-014-6005-z.

[4] G.F. White, M.J. Edwards, L. Gomez-Perez, D.J. Richardson, J.N. Butt, T.A. Clarke, Chapter Three - Mechanisms of Bacterial Extracellular Electron Exchange, in: R.K. Poole

(Ed.), Adv. Microb. Physiol., Academic Press, 2016: pp. 87–138. https://doi.org/10.1016/bs.ampbs.2016.02.002.

[5] N.L. Costa, T.A. Clarke, L.-A. Philipp, J. Gescher, R.O. Louro, C.M. Paquete, Electron transfer process in microbial electrochemical technologies: The role of cell-surface exposed conductive proteins, Bioresour. Technol. 255 (2018) 308–317. https://doi.org/10.1016/j.biortech.2018.01.133.

[6] A. Kumar, L.H.-H. Hsu, P. Kavanagh, F. Barrière, P.N.L. Lens, L. Lapinsonnière, J.H. Lienhard V, U. Schröder, X. Jiang, D. Leech, The ins and outs of microorganism–electrode electron transfer reactions, Nat. Rev. Chem. 1 (2017) 0024. https://doi.org/10.1038/s41570-017-0024.

[7] C.M. Paquete, B.M. Fonseca, D.R. Cruz, T.M. Pereira, I. Pacheco, C.M. Soares, R.O. Louro, Exploring the molecular mechanisms of electron shuttling across the microbe/metal space, Front. Microbiol. 5 (2014) 318. https://doi.org/10.3389/fmicb.2014.00318.

[8] B.M. Fonseca, C.M. Paquete, S.E. Neto, I. Pacheco, C.M. Soares, R.O. Louro, Mind the gap: cytochrome interactions reveal electron pathways across the periplasm of Shewanella oneidensis MR-1, Biochem. J. 449 (2013) 101–108. https://doi.org/10.1042/bj20121467.

[9] C.M. Paquete, R.O. Louro, Molecular details of multielectron transfer: the case of multiheme cytochromes from metal respiring organisms, Dalton Trans. 39 (2010) 4259–4266. https://doi.org/10.1039/B917952F.

[10] S. Beblawy, T. Bursac, C. Paquete, R. Louro, T.A. Clarke, J. Gescher, Extracellular reduction of solid electron acceptors by Shewanella oneidensis, Mol. Microbiol. 109 (2018) 571–583. https://doi.org/10.1111/mmi.14067.

[11] X. Jing, Y. Wu, L. Shi, C.L. Peacock, N.M. Ashry, C. Gao, Q. Huang, P. Cai, Outer Membrane c-Type Cytochromes OmcA and MtrC Play Distinct Roles in Enhancing the Attachment of Shewanella oneidensis MR-1 Cells to Goethite, Appl. Environ. Microbiol. 86 (2020) e01941-20. https://doi.org/10.1128/AEM.01941-20.

[12] A.C. Mitchell, L. Peterson, C.L. Reardon, S.B. Reed, D.E. Culley, M.R. Romine, G.G. Geesey, Role of outer membrane c-type cytochromes MtrC and OmcA in Shewanella oneidensis MR-1 cell production, accumulation, and detachment during respiration on hematite, Geobiology 10 (2012) 355–370. https://doi.org/10.1111/j.1472-4669.2012.00321.x.

[13] L. Shi, D.J. Richardson, Z. Wang, S.N. Kerisit, K.M. Rosso, J.M. Zachara, J.K. Fredrickson, The roles of outer membrane cytochromes of Shewanella and Geobacter in extracellular electron transfer, Environ. Microbiol. Rep. 1 (2009) 220–227. https://doi.org/10.1111/j.1758-2229.2009.00035.x.

[14] J. Oram, L.J.C. Jeuken, Tactic Response of Shewanella oneidensis MR-1 toward Insoluble Electron Acceptors, mBio 10 (2019) 02490-18. https://doi.org/10.1128/mbio.02490-18.

[15] S. Xu, A. Barrozo, L.M. Tender, A.I. Krylov, M.Y. El-Naggar, Multiheme Cytochrome Mediated Redox Conduction through Shewanella oneidensis MR-1 Cells, J. Am. Chem. Soc. 140 (2018) 10085–10089. https://doi.org/10.1021/jacs.8b05104.

[16] Y.-T. Zhang, Y. Zhang, L. Peng, Electrochemical fluorescence microscopy reveals insignificant long-range extracellular electron transfer in Shewanella oneidensis anodic

processes, Electrochim. Acta 398 (2021) 139305. https://doi.org/10.1016/j.electacta.2021.139305.

[17] G.W. Chong, S. Pirbadian, Y. Zhao, L.A. Zacharoff, F. Pinaud, M.Y. El-Naggar, Single molecule tracking of bacterial cell surface cytochromes reveals dynamics that impact long-distance electron transport, Proc. Natl. Acad. Sci. 119 (2022) e2119964119. https://doi.org/10.1073/pnas.2119964119.

[18] E. Lebègue, N.L. Costa, R.O. Louro, F. Barrière, Communication—Electrochemical Single Nano-Impacts of Electroactive Shewanella Oneidensis Bacteria onto Carbon Ultramicroelectrode, J. Electrochem. Soc. 167 (2020) 105501. https://doi.org/10.1149/1945-7111/ab9e39.

[19] H. Smida, F.-X. Lefèvre, C. Thobie-Gautier, M. Boujtita, C.M. Paquete, E. Lebègue, Single Electrochemical Impacts of Shewanella oneidensis MR-1 Bacteria for Living Cells Adsorption onto a Polarized Ultramicroelectrode Surface, ChemElectroChem 10 (2023) e202200906. https://doi.org/10.1002/celc.202200906.

[20] S. Goines, J.E. Dick, Review—Electrochemistry's Potential to Reach the Ultimate Sensitivity in Measurement Science, J. Electrochem. Soc. 167 (2019) 037505. https://doi.org/10.1149/2.0052003JES.

[21] S. Moussa, J. Mauzeroll, Review—Microelectrodes: An Overview of Probe Development and Bioelectrochemistry Applications from 2013 to 2018, J. Electrochem. Soc. 166 (2019) G25–G38. https://doi.org/10.1149/2.0741906jes.

[22] A. Sekretareva, Single-entity electrochemistry of collision in sensing applications, Sens. Actuators Rep. 3 (2021) 100037. https://doi.org/10.1016/j.snr.2021.100037.

[23] J. Luy, D. Ameline, C. Thobie-Gautier, M. Boujtita, E. Lebègue, Detection of Bacterial Rhamnolipid Toxin by Redox Liposome Single Impact Electrochemistry, Angew. Chem. Int. Ed. 61 (2022) e202111416. https://doi.org/10.1002/anie.202111416.

[24] H. Smida, C. Thobie-Gautier, M. Boujtita, E. Lebègue, Recent advances in single liposome electrochemistry, Curr. Opin. Electrochem. 36 (2022) 101141. https://doi.org/10.1016/j.coelec.2022.101141.

[25] H. Smida, A. Langlard, D. Ameline, C. Thobie-Gautier, M. Boujtita, E. Lebègue, Trends in single-impact electrochemistry for bacteria analysis, Anal. Bioanal. Chem. 415 (2023) 3717–3725. https://doi.org/10.1007/s00216-023-04568-z.

[26] J.W. Kim, G. Aruchamy, B.-K. Kim, Recent advances in single-entity electrochemistry for metal nanoparticle, nanodroplet, and bio-entity analysis, TrAC Trends Anal. Chem. 169 (2023) 117358. https://doi.org/10.1016/j.trac.2023.117358.

[27] B.M. Quinn, P.G. van't Hof, S.G. Lemay, Time-Resolved Electrochemical Detection of Discrete Adsorption Events, J. Am. Chem. Soc. 126 (2004) 8360–8361. https://doi.org/10.1021/ja0478577.

[28] Z. Deng, C. Renault, Detection of individual insulating entities by electrochemical blocking, Curr. Opin. Electrochem. 25 (2021) 100619. https://doi.org/10.1016/j.coelec.2020.08.001.

[29] A.T. Ronspees, S.N. Thorgaard, Blocking electrochemical collisions of single E. coli and B. subtilis bacteria at ultramicroelectrodes elucidated using simultaneous fluorescence microscopy, Electrochim. Acta 278 (2018) 412–420. https://doi.org/10.1016/j.electacta.2018.05.006.

[30] E.Z. Liu, S. Rivalta Popescu, A. Eden, J. Chung, B. Roehrich, L. Sepunaru, The role of applied potential on particle sizing precision in single-entity blocking electrochemistry, Electrochim. Acta 472 (2023) 143397. https://doi.org/10.1016/j.electacta.2023.143397.

[31] Q. Wang, J. Lin, S. Li, H. Tian, D. Zhang, Q. Xin, Label-Free Detection of Single Living Bacteria: Single-Entity Electrochemistry Targeting Metabolic Products, Anal. Chem. 95 (2023) 13082–13090. https://doi.org/10.1021/acs.analchem.3c01517.

[32] J.Y. Lee, B.-K. Kim, M. Kang, J.H. Park, Label-Free Detection of Single Living Bacteria via Electrochemical Collision Event, Sci. Rep. 6 (2016) 30022. https://doi.org/10.1038/srep30022.

[33] G. Gao, D. Wang, R. Brocenschi, J. Zhi, M.V. Mirkin, Toward the Detection and Identification of Single Bacteria by Electrochemical Collision Technique, Anal. Chem. 90 (2018) 12123–12130. https://doi.org/10.1021/acs.analchem.8b03043.

[34] Y.-S. Xu, T. Zheng, X.-Y. Yong, D.-D. Zhai, R.-W. Si, B. Li, Y.-Y. Yu, Y.-C. Yong, Trace heavy metal ions promoted extracellular electron transfer and power generation by Shewanella in microbial fuel cells, Bioresour. Technol. 211 (2016) 542–547. https://doi.org/10.1016/j.biortech.2016.03.144.

[35] A.D. Corts, L.C. Thomason, R.T. Gill, J.A. Gralnick, A new recombineering system for precise genome-editing in Shewanella oneidensis strain MR-1 using single-stranded oligonucleotides, Sci. Rep. 9 (2019) 1–10. https://doi.org/10.1038/s41598-018-37025-4.

[36] J.-W. Wu, I.-S. Ng, Biofabrication of gold nanoparticles by Shewanella species, Bioresour. Bioprocess. 4 (2017) 50. https://doi.org/10.1186/s40643-017-0181-5.

[37] L. Gao, X. Lu, H. Liu, D. Zhang, Mediation of Extracellular Polymeric Substances in Microbial Reduction of Hematite by Shewanella oneidensis MR-1, Front. Microbiol. 10 (2019) 575. https://doi.org/10.3389/fmicb.2019.00575.

[38] W. Ng, Zeta Potential of Escherichia Coli DH5α Grown in Different Growth Media, J. Environ. Sci. Public Health 5 (2021) 479–489. https://doi.org/10.26502/jesph.96120145.

[39] J.E. Dick, C. Renault, A.J. Bard, Observation of Single-Protein and DNA Macromolecule Collisions on Ultramicroelectrodes, J. Am. Chem. Soc. 137 (2015) 8376–8379. https://doi.org/10.1021/jacs.5b04545.

[40] Z. Deng, R. Elattar, F. Maroun, C. Renault, In Situ Measurement of the Size Distribution and Concentration of Insulating Particles by Electrochemical Collision on Hemispherical Ultramicroelectrodes, Anal. Chem. 90 (2018) 12923–12929. https://doi.org/10.1021/acs.analchem.8b03550.

[41] R. Gao, M.A. Edwards, J.M. Harris, H.S. White, Shot noise sets the limit of quantification in electrochemical measurements, Curr. Opin. Electrochem. 22 (2020) 170–177. https://doi.org/10.1016/j.coelec.2020.05.010.

Graphical abstract

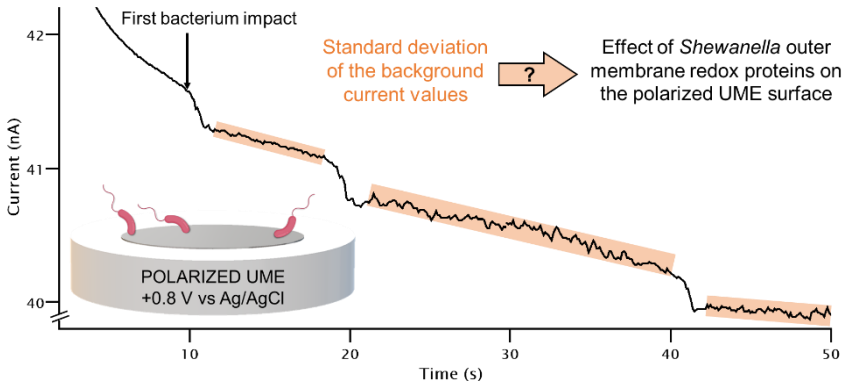

Highlights

- Blocking impacts electrochemistry of *Shewanella oneidensis* electroactive bacteria
- Chronoamperometry at the oxidation potential of the ferrocyanide redox probe
- Current step signals related to bacteria adsorption on the microelectrode surface
- Data analysis of the standard deviation values of the background current values
- Adhesion of *Shewanella* bacteria related to their outer membrane *c*-type cytochromes